MEDICAL SCIENCE MONITOR

LAB/IN VITRO RESEARCH

e-ISSN 1643-3750
© Med Sci Monit, 2017; 23: 2674-2683
DOI: 10.12659/MSM.904810

Received: 2017.04.11
Accepted: 2017.04.26
Published: 2017.06.01

Estrogen Receptor Mediates the Radiosensitivity of Triple-Negative Breast Cancer Cells

Authors' Contribution:
Study Design A
Data Collection B
Statistical Analysis C
Data Interpretation D
Manuscript Preparation E
Literature Search F
Funds Collection G

ABCDEFG 1,2 Xingxing Chen*
BCEF 1,3 Ningyi Ma*
CDEF 1,2 Zhirui Zhou*
BCF 4 Ziliang Wang
DE 1,2 Qunchao Hu
CE 1,2 Jurui Luo
DF 1,2 Xin Mei
DE 1,2 Zhaozhi Yang
EF 1,2 Li Zhang
DF 1,2 Xiaofang Wang
ADE 1,2 Yan Feng
AEG 1,2 Xiaoli Yu
AEF 1,2 Jinli Ma
AEG 1,2 Xiaomao Guo

1 Department of Radiation Oncology, Fudan University Shanghai Cancer Center, Shanghai, P.R. China
2 Department of Oncology, Shanghai Medical College, Fudan University, Shanghai, P.R. China
3 Department of Radiation Oncology, Shanghai Proton and Heavy Ion Center, Shanghai, P.R. China
4 Cancer Institutions, Fudan University Shanghai Cancer Center, Fudan University, Shanghai, P.R. China

* Equal contributors

Corresponding Authors: Xiaomao Guo, e-mail: guoxm1800@163.com, and Jinli Ma, e-mail: jinli.ma@aliyun.com

Source of support: This study was funded in full by the National Natural Science Foundation of China (grant numbers 81602668, 81402525, and 81372430) and Shanghai Sailing Program (grant number 16YF1401700)

Background: This study aimed to evaluate differences in the radiosensitivities of triple-negative breast cancer (TNBC) and luminal-type breast cancer cells and to investigate the effects of estrogen receptor (ER) expression on the biological behaviors of the cells.

Material/Methods: Colony-forming assays were performed to detect differences in radiosensitivities in breast cancer cell lines. Gene transfection technology was used to introduce the expression of ERα in TNBC cells to compare the difference in radiosensitivity between the TNBC cells and ERα transfected cells. CCK-8 assays were used to observe changes in the proliferation of TNBC cells after ERα transfection. Immunofluorescence was used to detect the number of γH2AX foci in nuclei. Flow cytometry was used to detect changes in cell cycle distribution and apoptosis. Western blotting was used to detect changes in autophagy-associated proteins.

Results: The radioresistance of the TNBC cell line MDA-MB-231 (231 cells) was greater than that of ERα-positive luminal-type breast cancer cell line MCF-7. Moreover, 231 cell proliferation and radioresistance decreased after ERα transfection. Interestingly, ERα-transfected 231 cells showed increased double-stranded breaks and delayed repair compared with 231 cells, and ERα-transfected 231 cells showed increased G_2/M phase arrest and apoptosis after irradiation compared with those in 231 cells. ERα transfection in 231 cells reduced autophagy-related protein expression, suggesting that autophagy activity decreased in 231 ER-positive cells after irradiation.

Conclusions: TNBC cells were more resistant to radiation than luminal-type breast cancer cells. ERα expression may have major roles in modulating breast cancer cell radiosensitivity.

MeSH Keywords: Estrogen Receptor alpha • Radiation • Transfection • Triple Negative Breast Neoplasms

Full-text PDF: http://www.medscimonit.com/abstract/index/idArt/904810

3923 — 8 29

Indexed in: [Current Contents/Clinical Medicine] [SCI Expanded] [ISI Alerting System] [ISI Journals Master List] [Index Medicus/MEDLINE] [EMBASE/Excerpta Medica] [Chemical Abstracts/CAS] [Index Copernicus]

Background

During the past 30 years, mortality rates in Chinese women with breast cancer have shown a gradual increase, making breast cancer a major cause of death in women [1]. Radiotherapy is an important procedure in the comprehensive treatment of breast cancer, it helps to reduce the frequency of distant metastasis and the mortality rate by blocking the local recurrence of breast cancer [2–4]. Many studies have shown that the local recurrence rate of triple-negative breast cancer (TNBC) is significantly higher than that of estrogen receptor (ER)-positive breast cancer [5], and negative ER status of breast cancer negatively influenced local recurrence rates [6], potentially owing to the different biological characteristics of these types of cancer cells. However, radiation resistance of TNBC may results in higher local recurrence rates. In Denmark, a large prospective meta-analysis supported this hypothesis [7]; patients with breast cancer were classified according to the molecular typing of ER and human epidermal growth factor receptor 2, and the results showed that the locoregional control benefit for TNBC by radiotherapy was significantly less than that for ER-positive luminal-type breast cancer. Thus, these results suggested that TNBC may be more radioresistant than ER-positive breast cancer. In addition, ER expression in luminal-type breast cancer may result in relative radiosensitivity.

As a major indicator of molecular typing, ER plays an important role in the development and progression of breast cancer. ER includes the ERα and ERβ subtypes [8], which are encoded by different genes; these genes share homology in some functional domains. The regulation of ER function is mainly mediated by the ERα subtype. ERα is mainly activated through the nuclear genome action system. This system includes estrogen-dependent, estrogen-independent, and estrogen-independent responsive element transcription pathways [9]. ER can also be activated by a nongenomic mechanism in which ER activates mitogen-activated protein kinase and AKT signaling pathways for signal transduction through "cross-talk" with insulin receptor substrate-1, Shc, and phosphoinositol 3-kinase [9,10]. After being activated by different pathways, ERα will activate the transcription of cell proliferation-associated genes to stimulate cell proliferation and invasion and inhibit apoptosis, thereby promoting the progression of breast cancer [11].

Although TNBC and luminal-type breast cancer differ in terms of local recurrence risks and radiotherapy efficacy [7,12,13], the radiobiological basis of these differences is not clear. Moreover, despite several basic studies of ERα and radiosensitivity, it is still unclear whether differences in ERα expression may cause differences in efficacy. Accordingly, in this study, we aimed to verify differences in radiosensitivity between breast cancer cell lines (MCF-7 and MDA-MB-231 cells) with different levels of ERα expression *in vitro*. Additionally, ERα was introduced into a TNBC cell line, MDA-MB-231 (231 cells), to observe changes in biological characteristics and radiosensitivity.

Material and Methods

Cell culture and cell irradiation methods

Human breast cancer cell lines MCF-7 (ATCC HTB-22) and MDA-MB-231 (ATCC HTB-26) were provided by the Breast Cancer Institute, Cancer Hospital, Fudan University. They were originally purchased from the American Type Culture Collection (ATCC, Manassas, USA). The MCF-7 cells were ER^+ and $HER2^-$, and the MDA-MB-231 cells were ER^- and $HER2^-$. The MDA-MB-231 cells were cultured in RPMI 1640 medium, and the MCF-7 cells were cultured in Dulbecco's modified Eagle's medium (DMEM). All culture media were supplemented with 10% fetal bovine serum, 100 U/mL penicillin, and 100 mg/mL streptomycin. Both cell lines were grown as attached cultures at 37°C in a humidified atmosphere containing 5% CO_2. During irradiation, the culture flasks were placed flat on a treatment bed on the top of a plexiglass plate with a thickness of 1.3 cm. Irradiation was performed using a linear accelerator (Siemens, Munich, Germany) with 6 MV-X ray irradiation and a source skin distance of 100 cm. The angle of the accelerator during irradiation was 180°, and the rays entered through the bottom of the flask. The actual dose absorption rate was 3–5 Gy/min measured using a dosimeter before irradiation.

Construction and identification of the ERα-expressing plasmid pBabe-ERα-puro

Genomic RNA was extracted from MCF-7 cells, and cDNA was synthesized using reverse transcription polymerase chain reaction (RT-PCR). Primers were designed based on the whole sequence of the *ERα* gene (1788 bp). The upstream primer sequence was 5'-C**GGGATCC**ATGACCATGACCCTCCACAC-3', and the downstream primer sequence was 5'-CG**GAATTC** TCAGACCGTGGCAGGGAAACCC-3'. According to the enzyme digestion sites in the vector, corresponding enzyme digestion sites were designed on the upstream and downstream primers. The upstream primer contained a *BamH*I digestion site (GGATCC), and the downstream primer had an *EcoR*I digestion site (GAATCC). The PCR primers were synthesized by the Beijing Genomics Institute (BGI, Beijing, China). MCF-7 cDNA was used as the template to amplify the ERα cDNA target fragment using PCR. The recovered target product and the empty vector were double digested with *BamH*I and *EcoR*I restriction endonucleases. The retroviral pBabe-puro vector was a gift from Professor Gong Yang at the Experimental Research Center of the Fudan University Cancer Center, the double digested target fragment and the vector were ligated, and 10 µL of the ligation product was used for the transformation step. The transformed and

Indexed in: [Current Contents/Clinical Medicine] [SCI Expanded] [ISI Alerting System] [ISI Journals Master List] [Index Medicus/MEDLINE] [EMBASE/Excerpta Medica] [Chemical Abstracts/CAS] [Index Copernicus]

amplified recombinant plasmid was extracted using a plasmid DNA midi-prep reagent kit (Tiangen Biotech, Beijing, China). The purified recombinant plasmid was identified by the double-enzyme digestion and was used for future experiments.

One hour before transfection, cells were cultured in fresh DMEM containing 0.05 mM chloroquine. After transfection, the cells were incubated in a 37°C incubator for 18–22 h, the culture medium was replaced, and the cells were transferred to a 32°C incubator to increase viral titers. At 48 h after transfection, the supernatant of the Phoenix cells was collected, centrifuged at 1500 rpm for 5 min to remove cell debris, and filtered through a 0.44-μm filter to obtain fresh virus. Infection was performed in a 37°C incubator for 48–72 h, and the cells could be repeatedly infected. After infection, the culture medium was changed twice, and the cells were transferred to 37°C. Puromycin selection was then performed. The 231 cells infected with virus were selected using puromycin for 3 weeks; the maintenance concentration was used for selection and amplification. Visible positive colonies, which consisted of cells stably transfected with the *ERα* gene, were selected. Total cellular protein was collected, and ERα expression in the stably transfected cells was identified using western blotting.

Determination of cell survival curves after irradiation

After cells in the logarithmic growth phase were irradiated with X-rays (0, 1, 2, 4, 6, or 8 Gy), they were harvested and counted immediately. According to the expected number of colony (30–100), the amount of single-cell suspension of each sample for inoculation was confirmed. Cells were inoculated into each of three 25-cm^2 culture flasks. Next, the cells were placed in an incubator for 12–14 days. After the formation of colonies, the cells were fixed in 4% paraformaldehyde. The colonies were then stained with 0.5% methylene blue for 15–30 min. Colonies containing at least 50 cells were counted using a stereomicroscope. The average number of colonies formed after each dose was calculated. The linear-quadratic model was used for fitting the survival curves [14] and for calculating the radiobiological parameters.

Detection of differences in the proliferation of cells *in vitro* using Cell Counting Kit-8 (CCK-8) assays

Cells in the logarithmic growth phase were collected and inoculated into 6 wells of a 96-well plate. A blank control was used for zeroing the spectrophotometer. Cells were continuously cultured, and cell proliferation was assessed at 0, 12, 24, 48, 72, 96, 120, 144, and 168 h after cell attachment using a CCK-8 reagent kit (Dojindo Molecular Technologies, Inc., Rockville, USA). The absorbance value of each well was detected at 450 nm using a microplate reader. Cell growth curves were plotted using time as the horizontal axis and absorbance value as the vertical axis.

Cellular immunofluorescence detection

Cells in the logarithmic growth phase were inoculated onto clean coverslips in 24-well plates at 2–5×10^4 cells/well. After 24 h, the cells were treated and harvested at different times after irradiation. Immunofluorescence staining was performed according to the following steps. First, cells were washed with phosphate-buffered saline (PBS) and fixed in 4% paraformaldehyde at room temperature for 10 min. After being washed with PBS, the cell membranes were permeabilized in 0.3% Triton X-100 at room temperature for approximately 5 min. After washing with PBS, the cells were blocked in 1% bovine serum albumin (BSA) at room temperature for approximately 60 min or at 37°C overnight. The horseradish peroxidase (HRP)-labeled primary antibody was diluted in 1% BSA according to the manufacturer's instructions (1: 100–1: 2000) and added to the wells in the dark. After incubation in a moisture box at 4°C overnight, the cells were washed with PBS. Any excess water on the coverslips was aspirated, and mounting fluid containing 5 μg/mL 4',6-diamidino-2-phenylindole (DAPI) was used for mounting. Cells were stored at 4°C in the dark or sent for observation with an immunofluorescence microscope. The same parameters were used for detection of each sample. The double-blind method was used to count the foci formed in each nucleus. More than 50 cells were counted. The average number of foci in each nucleus was calculated.

Analysis of the cell cycle using propidium iodide (PI) single staining

Cells were dissociated at designated time points and counted. Cells (5–10×10^5) were placed in a 15-mL centrifuge tube, centrifuged at 1500 rpm for 5 min, and washed twice with cold PBS; the final pellet was resuspended using a 100-μL pipette tip. Then, 1 mL of precooled (–20°C) 70% ethanol was added with vortexing. The cells were fixed in a –20°C refrigerator for at least 2 h. Before staining, the cells were centrifuged at room temperature at 1500 rpm for 5 min. After the ethanol was removed, the cells were washed twice with cold PBS, and the supernatant was discarded. The cells were resuspended using the residual liquid, 1 mL PI staining solution (50 μg/mL) was added, and the cells were incubated at room temperature in the dark for 30 min. Cell cycle data were collected using flow cytometry and associated software.

Detection of cell apoptosis using annexin V/PI double staining

Cells were dissociated at the designated time points and counted. Cells (5–10×10^5) were placed in a 15-mL centrifuge tube, washed twice with cold PBS, and centrifuged at 1500 rpm for 5 min. Next, 100 μL of binding buffer was added to resuspend the cells, 8 μL of staining solution (PI: annexin

Indexed in: [Current Contents/Clinical Medicine] [SCI Expanded] [ISI Alerting System] [ISI Journals Master List] [Index Medicus/MEDLINE] [EMBASE/Excerpta Medica] [Chemical Abstracts/CAS] [Index Copernicus]

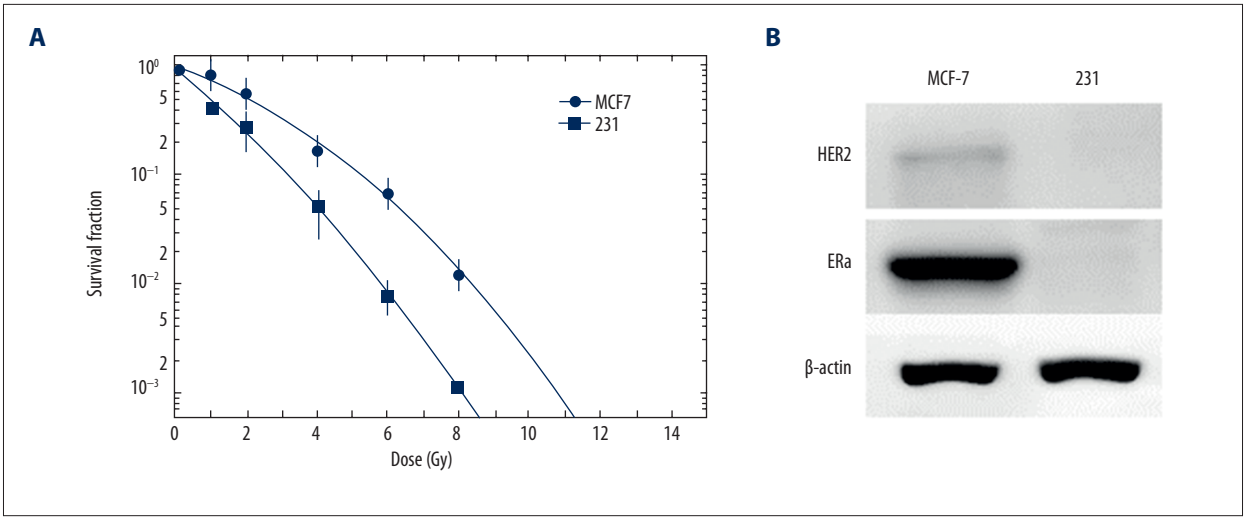

Figure 1. (**A**) Survival curves of 231 and MCF-7 cells. (**B**) Expression levels of endogenous HER2 and ERα in MCF-7 and 231 cells.

V-fluorescein isothiocyanate [FITC]=1: 1) was added, and the mixture was incubated at room temperature in the dark for 15–30 min. Samples were evaluated within 1 h. After the cells were stained, 400 µL of binding buffer was added and mixed well. The cells were analyzed using a flow cytometer, and the data were collected.

Detection of cellular protein changes using western blotting

Cells in the logarithmic phase were collected. After different treatments, the cells were detached using trypsin and collected for future usage. The collected cells were washed twice with precooled PBS and lysed in 100 µL lysis buffer (Beyotime Biotechnology, Shanghai, China) on ice for 30 min. Samples were centrifuged at 4°C and 18,500×*g* for 5 min. The supernatants were collected, and the total protein concentrations were determined using the BCA method. Twenty-five micrograms of protein from each group of samples was subjected to sodium dodecyl sulfate polyacrylamide gel electrophoresis, and samples were transferred onto a 0.22-µm polyvinylidene difluoride (PVDF) membrane and blocked in 5% skim milk for 1–2 h. The membranes were incubated with the primary antibodies at 4°C overnight, washed, and then incubated with HRP-labeled secondary antibodies. Enhanced chemiluminescent substrate reagents were mixed 1: 1 and added dropwise onto the PVDF membranes. The membranes were then incubated in the dark for 3–5 min. The protein bands were detected using ImageQuant LAS 400, and the fluorescence intensity was assessed. Digital images were analyzed for quantification of bands.

Statistical analysis

Statistical analysis was performed using SPSS19.0 software. The cell viability, survival fraction, apoptosis rate, and γH2AX foci are presented as means ± standard deviations. GraphPad Prism 5 (GraphPad software, La Jolla, USA) was used for analysis and for plotting the figures for the experimental data. Comparisons were carried out using independent sample T test. Differences with *P* values of less than 0.05 were considered statistically significant.

Results

Verification of differences in radiosensitivity among different breast cancer cell lines using colony formation assays

Cells with different ERα expression levels, i.e., MCF-7 ($ER\alpha^+$, $HER2^-$) and MDA-MB-231 cells (231 cells; $ER\alpha^-$, $HER2^-$), were selected for colony formation assays to verify their radiosensitivity. As shown in Figure 1A, the survival levels and shoulder regions of the survival curves of 231 cells at all the irradiation doses were higher than those of MCF-7 cells. These results suggested that 231 cells were more radioresistant than MCF-7 cells.

Verification of HER2 and ERα protein expression in different cell lines using western blotting

The expression levels of endogenous HER2 and ERα in MCF-7 and 231 cells were detected using western blotting. As shown in Figure 1B, MCF-7 cells were negative for HER2 and positive for ERα, and 231 cells were negative for both HER2 and ERα.

Indexed in: [Current Contents/Clinical Medicine] [SCI Expanded] [ISI Alerting System] [ISI Journals Master List] [Index Medicus/MEDLINE] [EMBASE/Excerpta Medica] [Chemical Abstracts/CAS] [Index Copernicus]

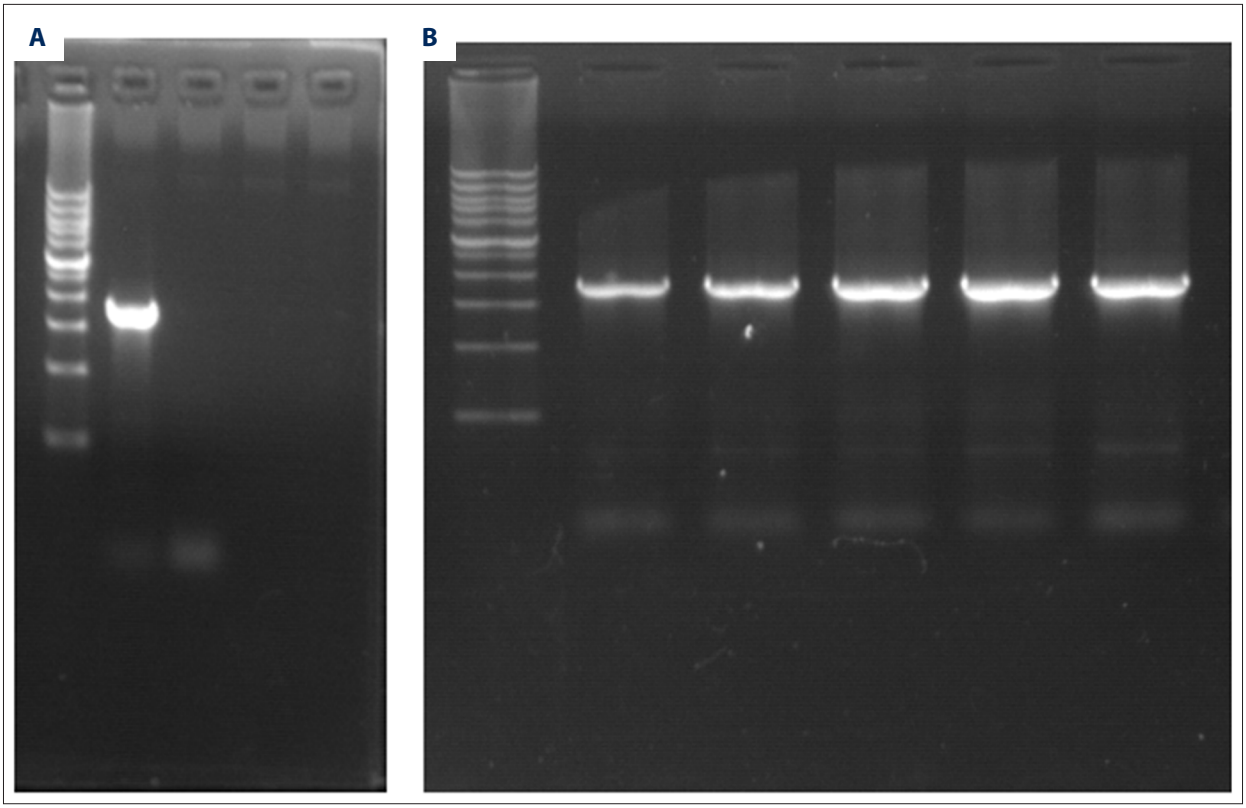

Figure 2. (**A**) Agarose gel electrophoresis of the ERα amplification fragment. (**B**) Electrophoresis of the double-enzyme digested recombinant plasmid.

Construction and characterization of a eukaryotic recombinant pBabe-puro-ERα plasmid expressing ERα

PCR was performed using MCF-7 cDNA as the template and the upstream and downstream primers for ERα. The required target gene fragment, ERα, was obtained (Figure 2A). The target gene in the gel was cut out, purified, and restriction digested using endonucleases *BamH*I and *EcoR*I (a map of the pBabe-puro expression plasmid is not shown). The empty pBabe-puro plasmid was also used for double-enzyme digestion with *BamH*I and *EcoR*I to linearize the vector. After double-enzyme digestion, the successful recombinant plasmid had an exogenous gene fragment with the expected size (1788 bp) and the vector fragment. This result indicated that a recombinant plasmid with an insertion of the ERα gene fragment was obtained and that the insertion direction was correct (Figure 2B). Recombinant plasmids identified by enzyme digestion were sequenced. The gene in the recombinant plasmid completely matched the original sequence of the human ERα gene in GenBank, indicating that the recombinant ERα-expressing plasmid, pBabe-puro-ERα, was successfully constructed (sequence results are not shown).

Construction and identification of 231 cells stably expressing ERα

The recombinant plasmid and an empty plasmid were transfected into Phoenix cells using the calcium phosphate transfection method. Viral particles with the target fragment or the empty viral particles were used to infect 231 cells in the logarithmic growth phase. Viruses packaged with green fluorescent protein (GFP) expression sequences were also used to infect Phoenix cells to observe the infection efficiency. Cells were observed with a fluorescence microscope after 48 h of infection. Green fluorescence could be observed in cells successfully transfected with the plasmid containing GFP expression sequences, the viral infection efficiency in this study was approximately 30%. Next, ERα expression in stably transfected ER231 cells was detected using western blotting (Figure 3A). The 231 cells transfected with the recombinant pBabe-puro-ERα plasmid successfully expressed the ERα protein with a molecular weight of 64 kDa. Neither the cells transfected with the empty pBabe-puro plasmid nor the parental cells showed ERα protein expression.

Indexed in: [Current Contents/Clinical Medicine] [SCI Expanded] [ISI Alerting System] [ISI Journals Master List] [Index Medicus/MEDLINE] [EMBASE/Excerpta Medica] [Chemical Abstracts/CAS] [Index Copernicus]

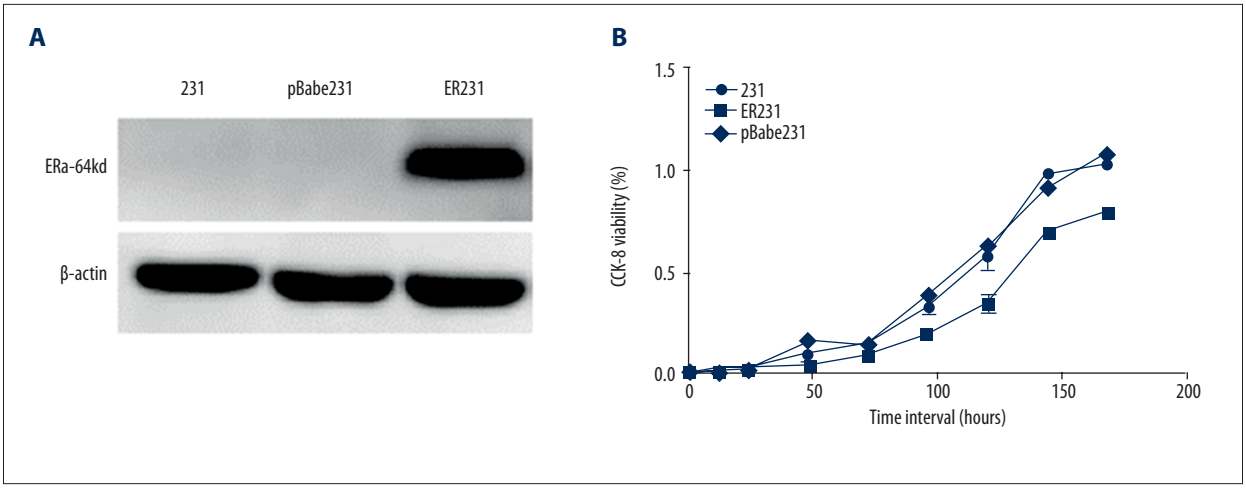

Figure 3. (**A**) Identification of ERα protein expression in stably transfected cell lines. (**B**) Growth curves of MDA-MB-231, ER231, and pBabe231 cells.

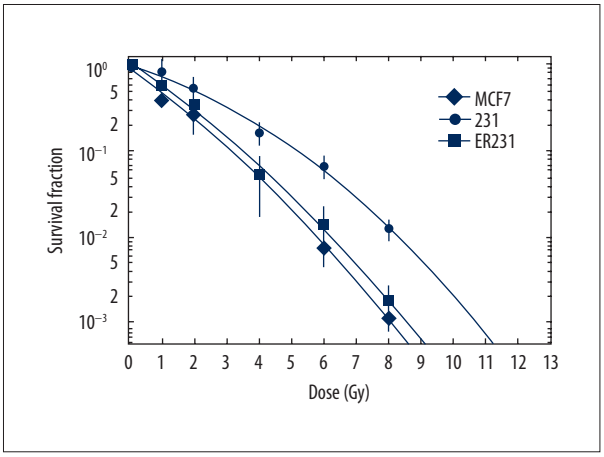

Figure 4. Survival of MDA-MB-231, ER231 and MCF-7 cells after exposure to different doses of radiation.

Changes in 231 cell proliferation after ERα transfection

The cell growth curves analyzed using the CCK-8 method are shown in Figure 3B. After 48 h of attachment, 231 cells entered the logarithmic growth phase, whereas ER231 cells entered the logarithmic growth phase at 72 h. Thus, the proliferation of ER231 cells was significantly slower than that of 231 cells, which was not significantly different from that of pBabe231 cells transfected with an empty vector. These results suggested that the proliferation of 231 cells decreased after ERα transfection.

Increased radiosensitivity of 231 cells after ERα transfection

The results of colony formation assays are shown in Figure 4. Compared with that of 231 cells, the shoulder region of the survival curve of irradiated ER231 cells was narrower, and the curve bent downward, suggesting increased radiosensitivity. The SF at 2Gy for 231, ER231 and MCF-7 was 0.53, 0.33, and 0.31, respectively. Therefore, these results suggested that the radiosensitivity of 231 cells increased after transfection with ERα.

Changes in the DSB frequency in nuclei of 231 cells after ERα transfection

After irradiation, the number of γH2AX foci in 231 and ER231 cells increased (Figure 5). The numbers of foci in the ER231 cells at all time points after irradiation were higher than in the 231 cells, especially significant at 1 and 2 hours after irradiation, respectively ($p<0.05$). These results suggested that ERα transfection delayed the repair of DNA DSB damage in 231 cells after irradiation and increased the amount of damage present.

Changes in the cell cycle of 231 cells after ERα transfection

To study changes in the cell cycle of ERα-transfected 231 cells after single-dose irradiation, cells at 16, 20, and 24 h after 6 Gy irradiation were harvested for cell cycle analysis. As shown in Figure 6, the distribution of cells in the cell cycle showed no significant differences between 231 and ER231 cells without irradiation. After irradiation, the 2 cell lines showed different degrees of G_2/M phase arrest compared with unirradiated cells. At 16, 20, and 24 h after irradiation, the proportion of cells arrested in the G_2/M phase was higher for ER231 cells than 231 cells. These results suggested that G_2/M phase arrest in ERα-transfected 231 cells increased after irradiation.

Changes in apoptosis in 231 cells after ERα transfection

The apoptosis of 231 cells and ER231 cells after irradiation is shown in Figure 7. After irradiation with 6 Gy, 231 cells and

Indexed in: [Current Contents/Clinical Medicine] [SCI Expanded] [ISI Alerting System] [ISI Journals Master List] [Index Medicus/MEDLINE] [EMBASE/Excerpta Medica] [Chemical Abstracts/CAS] [Index Copernicus]

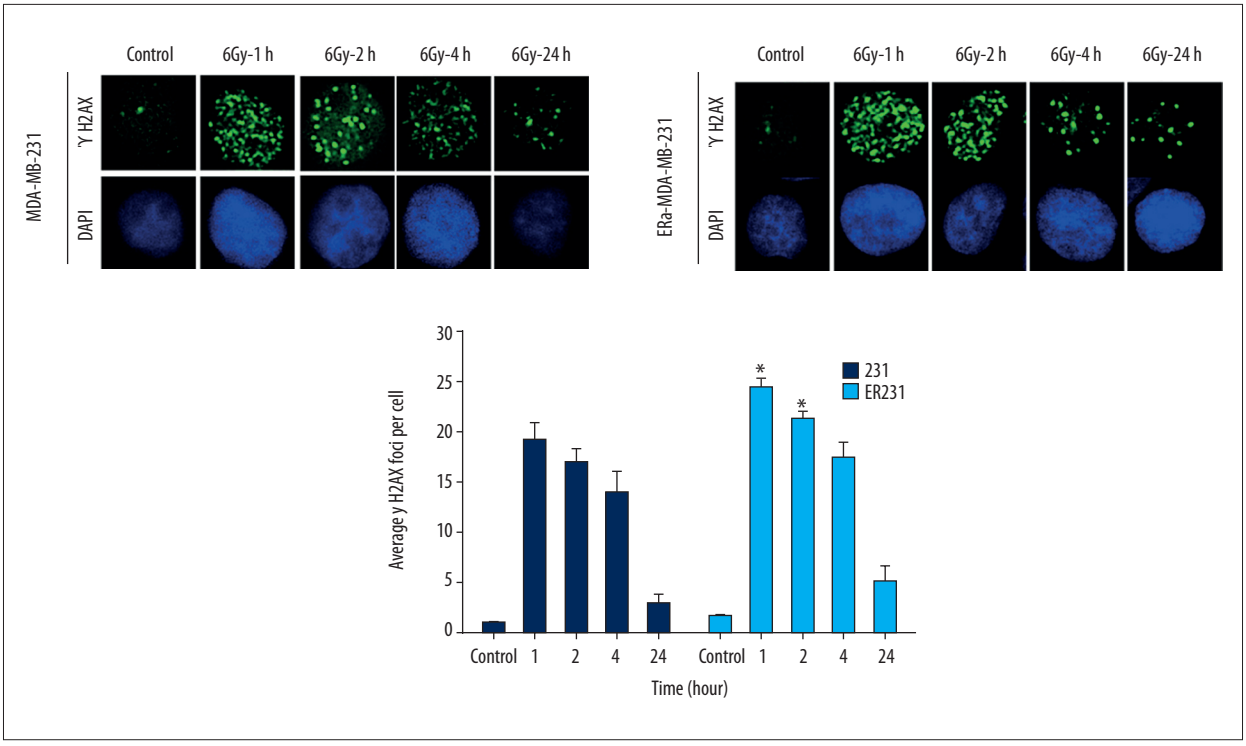

Figure 5. Changes in the number of γH2AX foci in each nucleus in 231 and ER231 cells after irradiation.

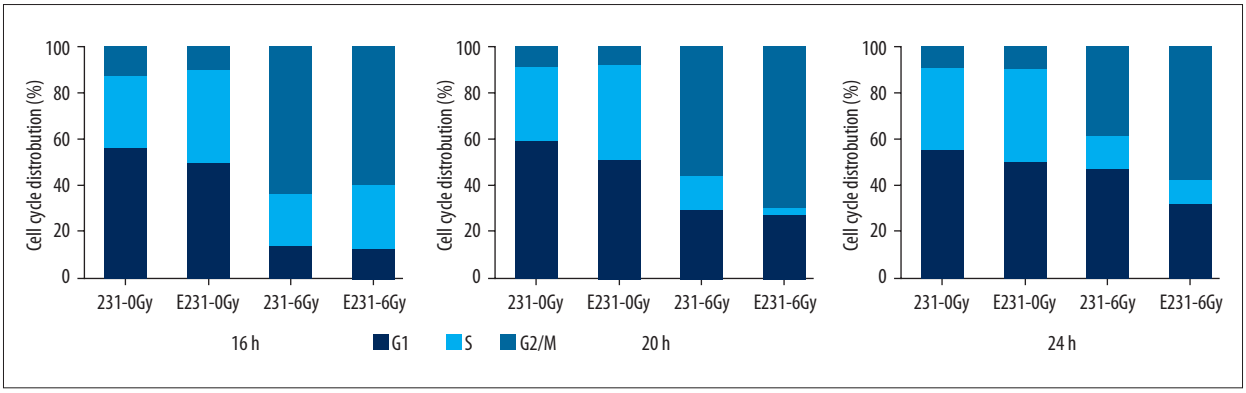

Figure 6. The cell cycle distributions of 231 and ER231 cells at different times after single-dose irradiation.

ER231 cells both exhibited early- and late-stage apoptosis in a time-dependent manner. The apoptosis was most obvious 96 h after irradiation. The levels of apoptosis in ER231 cells at all time points after irradiation were higher than those in 231 cells (early-stage apoptosis at 24 hours, $p=0.018$; late-stage apoptosis at 72 and 96 hours, $p<0.05$).

Changes in autophagy-associated protein expression in 231 cells after ERα transfection

The expression of cell autophagy-associated indicators is shown in Figure 8. The expression of autophagy-associated proteins increased after the 231 cells were irradiated, whereas the expression of autophagy-associated proteins slightly decreased in ER231 cells after irradiation. These results suggested that the autophagy level in ERα-transfected 231 cells decreased after irradiation, which could explain the radiosensitivity of breast cancer cells mediated by ERα.

Discussion

In this study, we aimed to verify differences in the radiosensitivities of various breast cancer cell lines and the relationship between radiosensitivity and ERα expression using molecular cloning technology to introduce ERα into TNBC 231 cells. The biological behaviors and changes in radiosensitivities of the TNBC cells after ERα transfection were observed. Cell

Indexed in: [Current Contents/Clinical Medicine] [SCI Expanded] [ISI Alerting System] [ISI Journals Master List] [Index Medicus/MEDLINE] [EMBASE/Excerpta Medica] [Chemical Abstracts/CAS] [Index Copernicus]

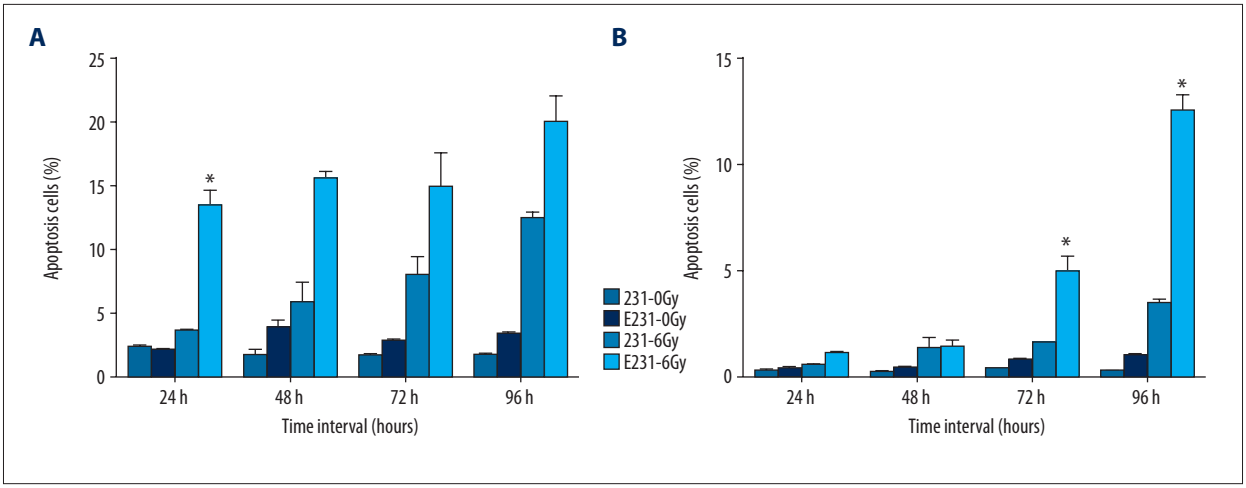

Figure 7. (**A**) Early-stage apoptosis in 231 and ER231 cells at different times after irradiation. (**B**) Late-stage apoptosis in 231 and ER231 cells at different times after irradiation.

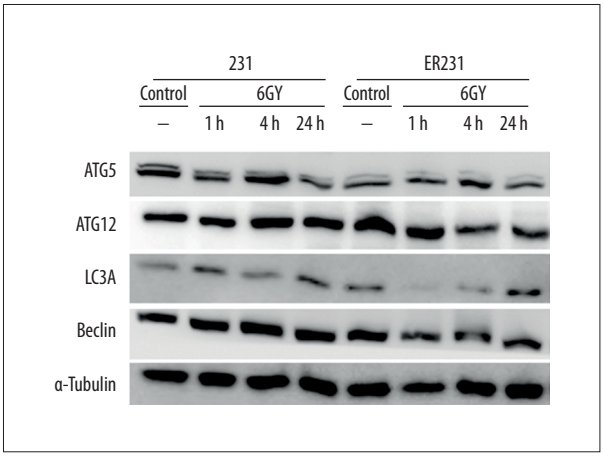

Figure 8. Expression of autophagy-associated proteins in 231 and ER231 cells after irradiation.

proliferation experiments showed that the proliferation ability of 231 cells decreased after transfection with ERα. Colony formation results showed that the radiosensitivity of ER231 cells was greater than that of the parental cells, which was close to that of ERα-positive luminal-type MCF-7 cells. The radiosensitivity of cells transfected with an empty vector was not significantly different than that of the parental cells. Thus, these results indicated that the radiosensitivity of TNBC cells increased after transfection with ERα.

Schmidberger et al. considered that in ER-positive cell lines, estrogen could interact with nuclear ER to cause the transcription of a series of cell cycle-associated genes [15], induce retinoblastoma protein phosphorylation, promote cell cycle progression, reduce the proportions of cells in the G_0 and S phases, cause cell death due to incomplete repair of DNA damage after irradiation, and increase the radiosensitivity of ER-positive cells. However, estrogen was not thought to affect ER-negative cells. Some studies used cDNA microarray technology to analyze differences in gene expression between TNBC and ER-positive cell lines [16,17]. The results showed that the expression levels of DNA repair genes, including *DNA-PK*, *HHR23A*, *HHR23B*, and *BRCA*, in TNBC cell lines were higher than those in ERα-positive cell lines. A study by Pedram et al. showed that the PI3K/AKT pathway is activated after estrogen interacts with the ER [18]. The activated AKT induces phosphorylation of TopBP1 protein at serine 1159, inhibits ATR activation after DNA damage, and delays DSB repair, thus increasing the level of damage after irradiation. These results suggested that cells with different ERα levels may have different damage repair abilities, resulting in differences in radiosensitivity.

It is well known that DNA is the target of irradiation damage, which includes damage such as single-strand breaks and DSBs. The presence of residual DSBs damage are associated with the γ-H2AX expression [19]. We observed a consistent decrease in the number of foci/nucleus from 1 to 24 h post-irradiation. There was higher in the number of foci positive for γ-H2AX/nucleus of ER231 cells than that of 231 cells, especially significant between 1 and 2 h post-irradiation. It indicated a more sustained inhibition of DNA repair for 231 cells with ERα transfection after irradiation, when compared with parental cells.

The difference in radiosensitivity was observed among G1, S and G2/M phase cells, of which G2/M phase cells are the most radiosensitive to irradiation. Furthermore, the G2/M phase arrest was observed in cells after irradiation, and the extent of the G2/M phase arrest are associated with the residual DNA damage after irradiation [20]. In our study, radiation-induced cell cycle changes were seen in both ER231 and 231 cells, including a time-dependent G1 and S phase reduction and accumulation of G2/M phase; and ERα transfection did further modify these cell cycle distributions. The increased radiosensitivity

Indexed in: [Current Contents/Clinical Medicine] [SCI Expanded] [ISI Alerting System] [ISI Journals Master List] [Index Medicus/MEDLINE] [EMBASE/Excerpta Medica] [Chemical Abstracts/CAS] [Index Copernicus]

of ER231 cells could also be explained with the modified cell cycle distribution compared to 231 cells.

Apoptosis, type I programmed cell death, was the main cell death mode observed after irradiation [21]. In our study, a high percentage of cells underwent apoptosis in a time-dependent manner after irradiation. And ERα transfection did cause additional increases in apoptosis in 231 cells, which could further promote the radiosensitivity. Autophagy, known as type II programmed cell death, plays an important role in the development and progression of tumors and is associated with drug resistance in tumor cells [22–24]. Autophagy is a newly recognized response to ionizing radiation in cells; however, reports on the relationship between autophagy and radiosensitivity are inconsistent. A report showed that autophagy was a major mechanism for the increase in radiosensitivity caused by AKT inhibitors and that autophagy promoted cell death after irradiation [25]. However, many other studies have indicated that autophagy may have protective effects on irradiated cells and could be associated with radioresistance in cells [26]. Although the specific pathway of radioresistance mediated by radiation-induced autophagy has not been identified, many studies have suggested that through reduction of radiation-induced cell damage, autophagy can promote cell escape, delay apoptosis, and increase cell survival, thus playing important roles in the mechanism of radioresistance in cells [27]; correspondingly, treatment with autophagy inhibitors has been shown to have the effect of increasing radiosensitivity in cells [28,29]. The results of our study showed that the autophagy-related protein level in ER231 cells after irradiation was lower than that in 231 cells, suggesting that the reduction of autophagy may play an important role in the increase of radiosensitivity in ER231 cells and that ERα may increase the radiosensitivity of cells by reducing autophagy.

Conclusions

The results of this study showed that the radioresistance of TNBC cell lines was greater than that of luminal-type breast cancer cell lines. This observation was validated by introducing ERα expression into a TNBC cell line. These results supported the observation from clinical studies that TNBC was relatively more radioresistant than luminal breast cancer.

Conflicts of interest

The authors declare that there are no conflicts of interest.

References:

1. Jia M, Zheng R, Zhang S et al: Female breast cancer incidence and mortality in 2011, China. J Thoracic Dis, 2015; 7(7): 1221–26
2. Clarke M, Collins R, Darby S et al: Effects of radiotherapy and of differences in the extent of surgery for early breast cancer on local recurrence and 15-year survival: An overview of the randomised trials. Lancet, 2005; 366(9503): 2087–106
3. Darby S, McGale P, Correa C et al: Effect of radiotherapy after breast-conserving surgery on 10-year recurrence and 15-year breast cancer death: Meta-analysis of individual patient data for 10,801 women in 17 randomised trials. Lancet, 2011; 378(9804): 1707–16
4. McGale P, Taylor C, Correa C et al: Effect of radiotherapy after mastectomy and axillary surgery on 10-year recurrence and 20-year breast cancer mortality: Meta-analysis of individual patient data for 8135 women in 22 randomised trials. Lancet, 2014; 383(9935): 2127–35
5. Chen X, Yu X, Chen J et al: Analysis in early stage triple-negative breast cancer treated with mastectomy without adjuvant radiotherapy: Patterns of failure and prognostic factors. Cancer, 2013; 119(13): 2366–74
6. Meattini I, Saieva C, Bastiani P et al: Impact of hormonal status on outcome of ductal carcinoma *in situ* treated with breast-conserving surgery plus radiotherapy: Long-term experience from two large-institutional series. Breast, 2017; 33: 139–44
7. Kyndi M, Sorensen FB, Knudsen H et al: Estrogen receptor, progesterone receptor, HER-2, and response to postmastectomy radiotherapy in high-risk breast cancer: The Danish Breast Cancer Cooperative Group. J Clin Oncol, 2008; 26(9): 1419–26
8. Dahlman-Wright K, Cavailles V, Fuqua SA et al: International Union of Pharmacology. LXIV. Estrogen receptors. Pharmacol Rev, 2006; 58(4): 773–81
9. Levin ER: Integration of the extranuclear and nuclear actions of estrogen. Mol Endocrinol, 2005; 19(8): 1951–59
10. Zivadinovic D, Gametchu B, Watson CS: Membrane estrogen receptor-alpha levels in MCF-7 breast cancer cells predict cAMP and proliferation responses. Breast Cancer Res, 2005; 7(1): R101–12
11. Yue W, Wang JP, Li Y et al: Effects of estrogen on breast cancer development: Role of estrogen receptor independent mechanisms. Int J Cancer, 2010; 127(8): 1748–57
12. Millar EK, Graham PH, O'Toole SA et al: Prediction of local recurrence, distant metastases, and death after breast-conserving therapy in early-stage invasive breast cancer using a five-biomarker panel. J Clin Oncol, 2009; 27(28): 4701–8
13. Nguyen PL, Taghian AG, Katz MS et al: Breast cancer subtype approximated by estrogen receptor, progesterone receptor, and HER-2 is associated with local and distant recurrence after breast-conserving therapy. J Clin Oncol, 2008; 26(14): 2373–78
14. Jones L, Hoban P, Metcalfe P: The use of the linear quadratic model in radiotherapy: A review. Australasian Phys Eng Sci Med, 2001; 24(3): 132–46
15. Schmidberger H, Hermann RM, Hess CF, Emons G: Interactions between radiation and endocrine therapy in breast cancer. Endocr Relat Cancer, 2003; 10(3): 375–88
16. Licznar A, Caporali S, Lucas A et al: Identification of genes involved in growth inhibition of breast cancer cells transduced with estrogen receptor. FEBS Lett, 2003; 553(3): 445–50
17. Skog S, He Q, Khoshnoud R et al: Genes related to growth regulation, DNA repair and apoptosis in an oestrogen receptor-negative (MDA-231) versus an oestrogen receptor-positive (MCF-7) breast tumour cell line. Tumour Biol, 2004; 25(1–2): 41–47
18. Pedram A, Razandi M, Evinger AJ et al: Estrogen inhibits ATR signaling to cell cycle checkpoints and DNA repair. Mol Biol Cell, 2009; 20(14): 3374–89
19. Siddiqui MS, François M, Fenech MF, Leifert WR: Persistent γH2AX: A promising molecular marker of DNA damage and aging. Mutat Res Rev Mutat Res, 2015; 766: 1–19
20. Thompson LH: Recognition, signaling, and repair of DNA double-strand breaks produced by ionizing radiation in mammalian cells: The molecular choreography. Mutat Res, 2012; 751(2): 158–246
21. Kim BM, Hong Y, Lee S et al: Therapeutic implications for overcoming radiation resistance in cancer therapy. Int J Mol Sci, 2015; 16(11): 26880–913
22. Hippert MM, O'Toole PS, Thorburn A: Autophagy in cancer: Good, bad, or both? Cancer Res, 2006; 66(19): 9349–51
23. Kondo Y, Kanzawa T, Sawaya R, Kondo S: The role of autophagy in cancer development and response to therapy. Nat Rev Cancer, 2005; 5(9): 726–34

Indexed in: [Current Contents/Clinical Medicine] [SCI Expanded] [ISI Alerting System] [ISI Journals Master List] [Index Medicus/MEDLINE] [EMBASE/Excerpta Medica] [Chemical Abstracts/CAS] [Index Copernicus]

24. Kondo Y, Kondo S: Autophagy and cancer therapy. Autophagy, 2006; 2(2): 85–90
25. Zhuang W, Qin Z, Liang Z: The role of autophagy in sensitizing malignant glioma cells to radiation therapy. Acta Biochim Biophys Sin, 2009; 41(5): 341–51
26. Luo J, Chen J, He L: mir-129-5p attenuates irradiation-induced autophagy and decreases radioresistance of breast cancer cells by targeting HMGB1. Med Sci Monit, 2015; 21: 4122–29
27. Abedin MJ, Wang D, McDonnell MA et al: Autophagy delays apoptotic death in breast cancer cells following DNA damage. Cell Death Differ, 2007; 14(3): 500–10
28. Apel A, Herr I, Schwarz H et al: Blocked autophagy sensitizes resistant carcinoma cells to radiation therapy. Cancer Res, 2008; 68(5): 1485–94
29. Chaachouay H, Ohneseit P, Toulany M et al: Autophagy contributes to resistance of tumor cells to ionizing radiation. Radiother Oncol, 2011; 99(3): 287–92

Indexed in: [Current Contents/Clinical Medicine] [SCI Expanded] [ISI Alerting System] [ISI Journals Master List] [Index Medicus/MEDLINE] [EMBASE/Excerpta Medica] [Chemical Abstracts/CAS] [Index Copernicus]